



Pergamon

Available online at www.sciencedirect.com

SCIENCE @ DIRECT®



Acta Materialia 51 (2003) 4965–4976

www.actamat-journals.com

Piezoelectric sensitivity of PbTiO₃-based ceramic/polymer composites with 0–3 and 3–3 connectivity

C.R. Bowen^a, V.Yu. Topolov^{b,*}

^a Materials Research Centre, Department of Engineering and Applied Science, University of Bath, BA2 7AY Bath, UK

^b Department of Physics, Rostov State University, Zorge street 5, 344090 Rostov-on-Don, Russia

Received 24 March 2003; received in revised form 25 April 2003; accepted 10 May 2003

Abstract

This paper describes the modelling and comparison of piezoactive composites of 0–3 and 3–3 geometry. Algorithms for the evaluation of effective elastic, piezoelectric and dielectric constants are proposed which can be used for the prediction of piezoelectric sensitivity and optimisation of properties. The hydrostatic piezoelectric voltage coefficient g_h , figure of merit $d_{33}g_{33}$ and hydrostatic figure of merit d_hg_h are calculated for PbTiO₃ based piezocomposites in which the anisotropy factor $-d_{33}/d_{31}$ of the piezoelectric phase can be varied from small to infinitely large values. Maxima of these parameters are determined and factors influencing piezoelectric sensitivity of the composites are analysed.

© 2003 Acta Materialia Inc. Published by Elsevier Ltd. All rights reserved.

Keywords: Composites; Modelling; Functional ceramics

1. Introduction

Piezoelectric sensitivity, such as charge generated per unit force or electric field generated per unit stress, is an important measurement of performance for heterogeneous ferroelectric materials. The need for increased piezoelectric sensitivity has led to the study [1–6], optimisation [7–9] and search for novel piezoelectric composites and structures. Recent work [10–12] has dealt with the prediction of electromechanical (elastic, piezoelectric and dielectric) properties of

piezoceramic/polymer composites having different microgeometry or α – β connectivity, defined by Newnham et al. [13,14]. The α term describes the connectivity of the primary piezoactive phase, while the β term corresponds to the connectivity of the secondary passive phase, which is often a polymer or air. These composites have been studied in an attempt to improve transducer performance, which is of importance for various applications such as hydrostatic hydrophones, acoustic sensors, medical and non-destructive testing transducers [14].

Depending on the transducer application, piezoelectric sensitivity is characterised by a set of parameters or figures of merit [1–4], such as the piezoelectric voltage coefficients (g_{33} and g_{31}),

* Corresponding author. Tel.: +7-8632-220885; fax: +7-8632-434044.

piezoelectric figure of merit ($d_{33} \cdot g_{33}$) and hydrostatic figure of merit (HFOM) $d_h \cdot g_h$, where the hydrostatic piezoelectric charge coefficient $d_h = d_{33} + 2d_{31}$, the hydrostatic piezoelectric voltage coefficient $g_h = d_h / \epsilon_{33}^T$ and ϵ_{33}^T is permittivity measured along the poling axis (OX_3) at constant stress.

Composites with large figures of merit offer considerable advantages over single crystal or monolithic polycrystalline ceramics in hydrophone and related underwater applications. A typical, and well researched, piezocomposite with large g_{33} , g_h , $d_{33} \cdot g_{33}$ and $d_h \cdot g_h$ values are 1–3 connectivity composites [1,3,5–9] which have piezoceramic rods, oriented along the poling axis, embedded in an elastically soft polymer matrix which is piezopassive or piezoactive. Further increases in the piezoelectric sensitivity of 1–3 composites can be achieved by a modification of the polymer matrix, for example, by forming laminated or porous structures in 1–2–2 [15] or 1–0–3 [16] composites, respectively.

While 1–3 composites have been well studied and characterised, similar parameters and figures of merit have not been studied or compared for other common two component piezocomposites, such as the 0–3 and 3–3 systems. A 0–3 composite consists of isolated piezoceramic particles in a continuous polymer matrix, while a 3–3 composite is made up of interpenetrating piezoceramic and polymer phases. In addition to composite architecture and connectivity, the effect of the anisotropy factor ($-d_{33}/d_{31}$) of the piezoelectric phase on composite parameters such as d_h , g_h and $d_h \cdot g_h$ has not been analysed in detail. This is surprising since the principal benefit of using the piezocomposite route is to develop a structure that displays a reduced d_{31} and therefore a higher $-d_{33}/d_{31}$ and d_h compared to the monolithic material.

This paper is aimed at the comparative study of 0–3 and 3–3 composites containing PbTiO_3 -based ceramics. The advantage of using PbTiO_3 -based piezocomposite ceramics is that, in addition to the varying the connectivity from 0–3 to 3–3, the anisotropy factor ($-d_{33}/d_{31}$) of the ceramic phase can also be varied from:

1. small values where the magnitude of d_{31} is large compared to d_{33} to,
2. infinitely large values where d_{31} is small compared to d_{33} .

The dependence of composite properties on ceramic piezoelectric properties, ceramic volume fraction, polymer properties, and composite geometry will be presented and comparisons are made to the more common 1–3 system.

2. Materials for 0–3 and 3–3 composites

Table 1 presents the elastic, piezoelectric and dielectric constants of the PbTiO_3 , $(\text{Pb}_{0.76}\text{Ca}_{0.24})\text{TiO}_3$ and $\text{Pb}(\text{Zr}_{1-x}\text{Ti}_x)\text{O}_3$ piezoceramics examined in this study, which were calculated according to an algorithm in [17]. It is known from experimental data on PbTiO_3 -based piezoceramics that the grains have a well-defined domain structure [21,22]. It is assumed in this work that the ceramic grains contain spherical grains split into 90° domains of two types with volume concentrations m_d and $1-m_d$. In the presence of these domain types, the internal stress is relieved and a lowering of the electric depolarization field is realised over the polydomain grain. In the first stage of our calculations, a complete set of piezoelectric coefficients d_{ij}^p , elastic compliances s_{kl}^p and dielectric permittivities ϵ_{pp}^T of the polydomain single crystal is determined. These constants are evaluated as functions of the volume concentration of the two 90° domain types (i.e., m_d). For averaging, the 90° domains are assumed to be elements of a regular laminated domain structure and is divided by a planar domain wall through the ceramic grain. The averaging procedure is carried out by the method of piecewise uniform fields [21]. This method is based on using known single-domain crystal electromechanical constants and taking into account the boundary conditions for the electric and mechanical fields of adjacent 90° domains. The electromechanical interaction between the domains leads [17] to an appearance of excess components of the mechanical and electric fields (in addition to the fields applied at measurements). The excess fields, being averaged over the domain structure of the grains, are absent.

In the second stage, the averaging procedure by

Table 1
Elastic (s_{ij}^E , in 10^{-12} Pa $^{-1}$), piezoelectric (d_{3i} , in 10^{-12} m/V) and dielectric ($\epsilon_{33}^T/\epsilon_0$) constants of components for 0–3 and 3–3 composites

Component	s_{11}^E	s_{12}^E	s_{13}^E	s_{33}^E	d_{31}	d_{33}	$\epsilon_{33}^T/\epsilon_0$	Note
PbTiO ₃	6.12	-1.12	-1.12	6.12	-0.00228	0.0869	95.3	Calculated [17] for $\theta = 175^\circ$ and $m_d = 0.5$
	6.07	-1.08	-1.14	6.07	-0.0581	2.99	84.5	Calculated [17] for $\theta = 150^\circ$ and $m_d = 0.5$
	5.98	-1.03	-1.15	6.03	-0.0354	10.7	95.5	Calculated [17] for $\theta = 120^\circ$ and $m_d = 0.5$
	6.12	-1.12	-1.12	6.3	0.121	21.8	100	Calculated [17] for $\theta = 90^\circ$ and $m_d = 0.5$
	6.59	-1.5	-1.02	7.19	-0.128	38.4	112	Calculated [17] for $\theta = 55^\circ$ and $m_d = 0.5$
	6.69	-1.63	-0.97	7.49	-0.297	43.4	116	Calculated [17] for $\theta = 45^\circ$ and $m_d = 0.5$
	6.02	-1.14	-1.15	6.17	-0.00198	0.0996	150	Calculated [18] for $\theta = 175^\circ$ and $m_d = 0.5$
	5.98	-1.1	-1.17	6.12	-0.063	3.47	150	Calculated [18] for $\theta = 150^\circ$ and $m_d = 0.5$
	5.89	-1.05	-1.18	6.06	-0.169	12.7	150	Calculated [18] for $\theta = 120^\circ$ and $m_d = 0.5$
	6.02	-1.14	-1.15	6.34	-0.272	26.1	158	Calculated [18] for $\theta = 90^\circ$ and $m_d = 0.5$
(Pb _{0.76} Ca _{0.24})TiO ₃	6.45	-1.52	-1.06	7.26	-0.511	45.5	176	Calculated [18] for $\theta = 55^\circ$ and $m_d = 0.5$
	6.54	-1.66	-1.01	7.53	-0.546	50.8	182	Calculated [18] for $\theta = 45^\circ$ and $m_d = 0.5$

(continued on next page)

Table 1 (continued)

Component	s_{11}^E	s_{12}^E	s_{13}^E	s_{33}^E	d_{31}	d_{33}	$\epsilon_{33}^E/\epsilon_0$	Note
$\text{Pb}(\text{Zr}_{1-x}\text{Ti}_x)\text{O}_3$	6.15	-1.6	-1.66	6.31	-6.84	26.7	154	Calculated [18] for $x = 0.1$, $\theta = 45^\circ$ and $m_q = 0.5$
	6.66	-1.73	-1.8	6.88	-9.59	37.5	237	Calculated [18] for $x = 0.2$, $\theta = 45^\circ$ and $m_q = 0.5$
	6.85	-1.89	-1.99	7.07	-13.8	44.9	327	Calculated [18] for $x = 0.3$, $\theta = 45^\circ$ and $m_q = 0.5$
	7.46	-2.33	-2.49	7.68	-26.2	61.4	547	Calculated [18] for $x = 0.4$, $\theta = 45^\circ$ and $m_q = 0.5$
Modified PbTiO_3	7.5	-1.5	-1.1	8	-4.4	51	170	Experimental data [19]
PCR-62	9	-3.2	-3.2	8.6	-42	84	660	Experimental data [20]
PCR-63	9.8	-3.5	-2.7	9.8	-60	140	1170	Experimental data [20]
Elastomer	3300	-1480	-1480	3300	0	0	5	Experimental data [2]
Porous elastomer	4790	-1600	-1600	4790	0	0	3.52	Calculated for disk-like pores with $\alpha = 0.1$ and $m_p = 0.1$
	6420	-1650	-1650	6420	0	0	2.56	Calculated for disk-like pores with $\alpha = 0.1$ and $m_p = 0.2$
	17200	-2200	-2200	17200	0	0	1.51	Calculated for disk-like pores with $\alpha = 0.01$ and $m_p = 0.1$
	34500	-3100	-3100	34500	0	0	1.1	Calculated for disk-like pores with $\alpha = 0.01$ and $m_p = 0.2$

Note. The abbreviation "PCR" means "piezoceramic from Rostov-on-Don". The piezoceramics of the PCR group have been first processed and studied at the Rostov State University (Rostov-on-Don, Russia) [20].

the effective medium method [17,21] is carried out and electromechanical constants of piezoceramics are determined as functions of the maximum angle θ between the vectors $\mathbf{P}_\Sigma = m_d \mathbf{P}_{s1} + (1 - m_d) \mathbf{P}_{s2}$ of the spontaneous polarisation of grains and the poling field (\mathbf{E}) along OX_3 , where \mathbf{P}_{s1} and \mathbf{P}_{s2} are spontaneous polarization vectors of adjacent 90° domains, m_d is the volume concentration of the domains with \mathbf{P}_{s1} on condition that $(\mathbf{P}_{s1}, \hat{\mathbf{E}}) \leq (\mathbf{P}_{s2}, \hat{\mathbf{E}})$. The angle θ in Table 1 correlates with the piezoelectric remanent polarization (\mathbf{P}_R) in OX_3 and decreasing θ , the angle between the direction of spontaneous polarization and the poling field, increases \mathbf{P}_R [17]. In tetragonal piezoceramics, angles $\theta < 55^\circ$ or $\theta < 45^\circ$ cannot be achieved in single-domain or polydomain grains, respectively.¹ Experimental data for other modified PbTiO_3 materials are also presented in Table 1, along with compliance data of a variety of elastomers to be used as the matrix material. These materials were chosen as they provide a means to examine how the properties of the piezoelectric phase (such as d_{33} , d_{31} , $-d_{31}/d_{33}$, ϵ_{33}^T etc.) and polymer phase (s_{11} , ϵ_{33}^T etc.) influence the performance of 0–3 and 3–3 composites.

3. PbTiO_3 -based composites with 0–3 connectivity

This section considers the influence of piezoceramic volume fraction on the piezoelectric sensitivity of 0–3 based composites. The composite is represented by a set of cubic *Banno unit cells* [24,25], and each unit cell contains a piezoceramic inclusion surrounded by a matrix (Fig. 1). The inclusion is in the form of the rectangular parallelepiped and its length, width and height make up the t th, n th and h th parts of the Banno unit-cell edge, respectively as shown in Fig. 1.

The electromechanical constants of the piezoceramic and polymer components are averaged by

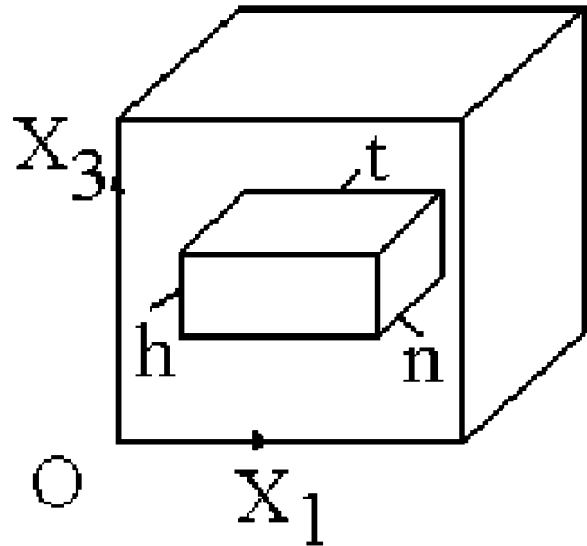


Fig. 1. Schematic representation of the cubic Banno unit cell for the 0–3 connectivity pattern.

a matrix method that has been applied to 2–2, 0–3 and 1–3 connectivity patterns [25,26]. The averaging procedure implicates the determination of the effective constants of a laminated piezoceramic–polymer structure by taking into account the electrical and mechanical boundary conditions at (i) $x_1 = \text{constant}$, (ii) $x_2 = \text{constant}$ and (iii) $x_3 = \text{constant}$ separately. As a result, the full set of effective elastic compliances s_{ab}^E , piezoelectric coefficients d_{ki} , and dielectric permittivities ϵ_{ff}^T of the composite can be calculated as a function of t , n and h which represent the piezoelectric particle length, width and breadth. These parameters characterise the volume fraction of the polymer matrix (m_{pol}), since $m_{\text{pol}} = 1 - tnh$.

The first calculations are related to 0–3 composites with cubic shaped inclusions embedded in the homogeneous matrix, such that $t = n = h$ in Fig. 1. Symmetry of this composite in the poled state is ∞ mm. Table 2 presents a summary of the maximum g_h and $d_{33} \cdot g_{33}$ of 0–3 composites with cubic inclusions of PbTiO_3 and $(\text{Pb}_{0.76}\text{Ca}_{0.24})\text{TiO}_3$ embedded in the elastomer in Table 1. Decreasing the angle θ and increasing the degree of remanent polarization \mathbf{P}_R of the piezoceramic component results in a monotonous increase of the maximum values of g_h and $d_{33} \cdot g_{33}$, as seen in Table 2. The

¹ Additional results of calculation of the effective electro-mechanical constants of the PbTiO_3 -based piezoceramics are published in [17,18,21,23]. For example, data on the effect of the 90° domain structure on piezoelectric coefficients d_{3j} have been shown in [21,23].

Table 2

Maxima of effective parameters g_h (in $10^{-3} \text{ V m}^{-1} \text{ Pa}^{-1}$) and d_{33}, g_{33} (in 10^{-12} Pa^{-1}) of the 0–3 composite “(Pb_{1-x}Ca_x)TiO₃—elastomer”

θ , deg	$x = 0$ (PbTiO ₃)				$x = 0.24$ (Pb _{0.76} Ca _{0.24} TiO ₃)			
	max g_h	t_1	max(d_{33}, g_{33})	t_2	max g_h	t_1	max(d_{33}, g_{33})	t_2
175	0.0575	0.27	1.16×10^{-5}	0.22	0.051	0.2	9.92×10^{-6}	0.19
150	2.00	0.27	0.0138	0.21	1.78	0.2	0.0121	0.19
120	7.23	0.27	0.177	0.21	6.54	0.2	0.162	0.19
90	14.3	0.27	0.694	0.21	13.1	0.2	0.65	0.18
55	23.4	0.25	1.93	0.21	21.2	0.2	1.73	0.18
45	25.8	0.23	2.37	0.21	23.2	0.19	2.08	0.18

Note. The concentration parameters t_1 and t_2 correspond to t value for maximal g_h and d_{33}, g_{33} , respectively.

maximum g_h and d_{33}, g_{33} tend to occur at particle sizes of $t = 0.18–0.27$. As θ approaches 45° the values of maximum g_h and d_{33}, g_{33} from Table 2 become comparable with experimentally measured parameters, namely $g_h = 27.2 \text{ mV m/N}$ and $d_{33}, g_{33} = 1.68 \text{ pPa}^{-1}$, for monolithic modified PbTiO₃ [19]. The concentration dependence of $d_h \cdot g_h$ has a slight maximum in a vicinity of $t = 0.2$, however the value of maximum $d_h \cdot g_h$ is two orders of magnitude lower than $d_h \cdot g_h = 1.15 \text{ p Pa}^{-1}$ of the monolithic modified PbTiO₃.

The next stage of our calculations is remove the constraint of cubic inclusions and consider the variation of all the concentration parameters $0 < (t, n, h) < 1$ of the 0–3 composite. Such a composite poled along the OX_3 axis is characterised by symmetry mm2, and its effective electromechanical constants obey the conditions below, where h_0 is constant and $0 < h_0 < 1$,

$$\begin{aligned} d_{ki}(t, n, h_0) &= d_{ki}(t', n', h_0) \\ s_{ab}^E(t, n, h_0) &= s_{ab}^E(t', n', h_0) \\ \varepsilon_{ff}^T(t, n, h_0) &= \varepsilon_{ff}^T(t', n', h_0) \end{aligned} \quad (1)$$

where $t' = n$ and $n' = t$. For example, $d_{33}(0.1, 0.8, 0.9) = d_{33}(0.8, 0.1, 0.9)$.

By variation of n and t , it is possible to establish maxima of g_h , d_{33}, g_{33} and $d_h \cdot g_h$ for the 0–3 particulate geometry. The values of these maxima increase with increasing h_0 (the height of the particle in Fig. 1) and in the limiting case of $h = 1$ the composite has 1–3 connectivity, where the absolute maxima of g_h , d_{33}, g_{33} and $d_h \cdot g_h$ are achieved.

From our evaluations, a difference between values of local maximum $g_h(t, n, 0.9)$ and the absolute maximum of g_h does not exceed 5%, and any trend is therefore typical of the concentration dependences of d_{33}, g_{33} and $d_h \cdot g_h$. Plots of the concentration dependences related to 0–3 composite with $h = 0.95$ and variables (t, n) are shown in Fig. 2. These composites display relatively high values of $g_h^c \approx 4g_h^m$ (Fig. 2a) and $d_{33}, g_{33}^c \approx 15d_{33}, g_{33}^m$ (Fig. 2b). The “c” superscript relates to the property of the piezocomposite and the “m” superscript relates to the properties of the monolithic piezoceramic. The location of the g_h and d_{33}, g_{33} maxima are realised at

1. $t \ll 1, n \rightarrow 1$ or
2. $n \ll 1, t \rightarrow 1$. (conditions 1)

The above conditions correspond to the use of “plate-like” or “fibre-like” piezoceramic inclusions having the least edge lying along one of the non-polar (OX_1 or OX_2) axes (Fig. 2a). The HFOM, $d_h \cdot g_h$, is characterised by a monotonous concentration dependence on both t and n as these concentration parameters are varied from 0.01 to 0.99, as shown in Fig. 2c. The largest HFOM remains two orders of magnitude lower than $d_h \cdot g_h$ of the bulk modified PbTiO₃ because 0–3 connectivity corresponds to isolated ceramic particles and a discontinuous distribution of the piezoceramic inclusions in the polymer matrix along the poling axis OX_3 ($h < 1$). At such a discontinuous distribution the effective piezoelectric coefficients d_{33} and d_h remain relatively small compared to the monolithic

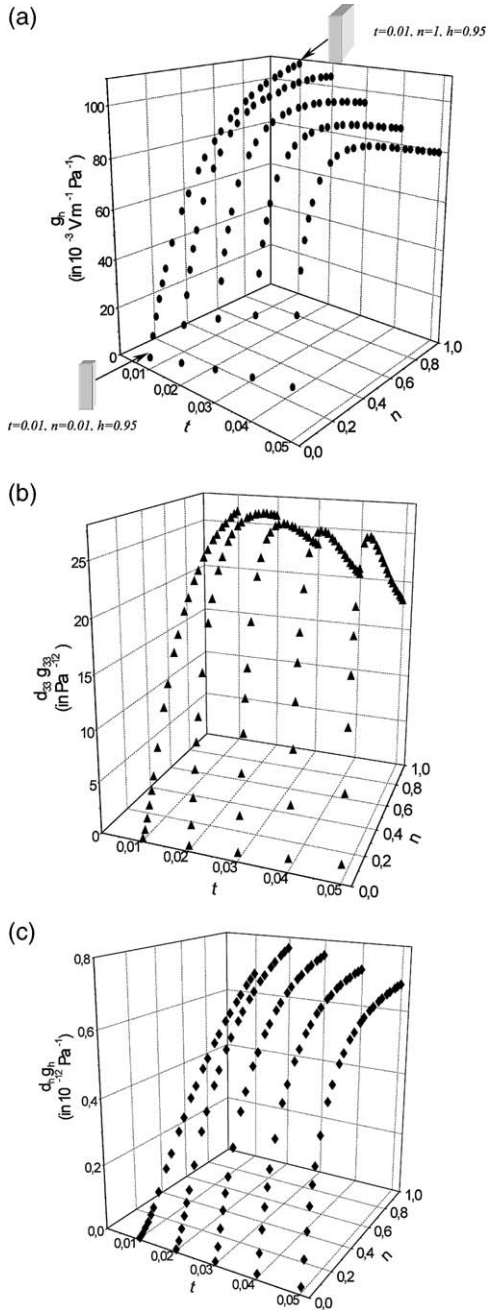


Fig. 2. Effective parameters g_h (a), $d_{33} \cdot g_{33}$ (b) and $d_h \cdot g_h$ (c) that characterise piezoelectric sensitivity of the 0–3 composite “modified PbTiO_3 piezoceramic—elastomer” with inclusions in the form of a rectangular parallelepiped (as shown in (a)). The concentration parameters are chosen as follows: $h = 0.95$, $0.01 \leq t \leq 0.05$ and $0.01 \leq n \leq 0.99$.

material and do not provide a large HFOM. A considerable difference between the $d_{33} \cdot g_{33}$ and $d_h \cdot g_h$ values at these conditions is accounted for by the small volume fraction of the piezoceramic. At low ceramic volume fractions the piezoelectric anisotropy ($-d_{33}/d_{31}$) of the ceramic is unable to influence a redistribution of internal electric and mechanical fields and promote an increase in the HFOM of the composite.

The final set of calculations is associated with an increase in piezoelectric sensitivity of the 0–3 composite by incorporating disk like porosity into the passive polymer matrix in an attempt to reduce the permittivity and compliance of the passive phase. A formation of randomly distributed disk-like air pores as shown in Fig. 3 which obey the condition,

$$(x_1 / a_1)^2 + (x_2 / a_1)^2 + (x_3 / a_3)^2 = 1 \quad (2)$$

with $\alpha_{sa} = a_3/a_1 \ll 1$ results in elongated pores normal to the poling axis and an increase in the s_{11} and $|s_{12}|$ elastic compliances [27]. This can be observed by comparison of the s_{11} and s_{12} constants of the “elastomer” and “porous elastomer” in Table 1. These elastic compliances are functions of porosity volume fraction m_p and the ratio of semi-axes α_{sa} . The disk-like porous structure of the polymer matrix becomes an important factor in achieving large increases in piezoelectric sensitivity. Table 3 shows g_h , $d_{33} \cdot g_{33}$ and $d_h \cdot g_h$ of a modified PbTiO_3 based “piezoceramic–porous

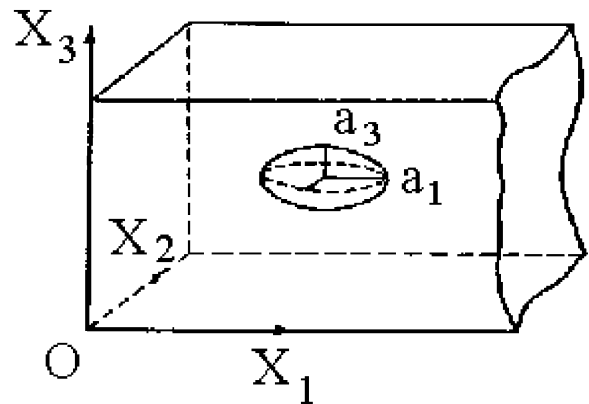


Fig. 3. Schematic representation of the 0–3 composite with a spheroidal pore. a_1 , $a_2 = a_1$ and a_3 are spheroid’s semi-axes being parallel to the coordinate axes OX_i .

Table 3

Maxima of effective parameters g_h (in $10^{-3} \text{ V m}^{-1} \text{ Pa}^{-1}$), $d_{33}g_{33}$ (in 10^{-12} Pa^{-1}) and $d_h g_h$ (in 10^{-12} Pa^{-1}) of the 0–0–3 composite “modified PbTiO_3 —porous elastomer”

Porosity t m_p		Max g_h at α_{sa} = 0.1	Max($d_{33}g_{33}$) at $\alpha_{sa} = 0.1$	Max($d_h g_h$) at $\alpha_{sa} =$ 0.1	Max g_h at $\alpha_{sa} =$ 0.01	Max($d_{33}g_{33}$) at α_{sa} = 0.01	Max($d_h g_h$) at α_{sa} = 0.01
0.1	0.03	354 (0.27)	38.1 (0.29)	5.77 (0.64)	1810 (0.07)	98.1 (0.10)	54.7 (0.10)
	0.05	342 (0.15)	38.2 (0.18)	5.10 (0.27)	1810 (0.04)	98.1 (0.06)	54.5 (0.06)
	0.1	332 (0.07)	38.3 (0.09)	4.65 (0.11)	1810 (0.02)	98.1 (0.03)	54.4 (0.03)
	0.2	328 (0.03)	38.3 (0.05)	4.45 (0.05)	1810 (0.009)	96.4 (0.02)	53.4 (0.02)
	0.3	326 (0.02)	38.2 (0.03)	4.39 (0.03)	1790 (0.002)	92.1 (0.02)	54.3 (0.007)
0.2	0.03	668 (0.16)	51.5 (0.22)	13.7 (0.26)	2910 (0.04)	147 (0.06)	99.1 (0.06)
	0.05	658 (0.09)	51.5 (0.13)	13.1 (0.15)	2910 (0.025)	147 (0.035)	99.1 (0.035)
	0.1	650 (0.05)	51.5 (0.07)	12.7 (0.07)	2900 (0.012)	147 (0.018)	99.0 (0.018)

Notes. (1) Piezoceramic inclusions are in the form of the rectangular parallelepiped with the concentration parameters $h = 0.95$, t being varied and n corresponding to maxima (see the optimal values of n in parentheses). (2) Disk-like air pore microgeometry is described by Eq. (2) and the volume fraction of these pores in the polymer component is expressed by porosity m_p .

polymer” composite with 0–0–3 connectivity and m_p values of 0.10 and 0.20 and α_{sa} values of 0.1 and 0.01. As was observed with the 0–3 composite with cubiform inclusions, the 0–0–3 composite is described by symmetry ∞mm . It should be noted that even at fairly low polymer porosity $m_p = 0.10$ and $\alpha_{sa} = 0.1$, the calculated values of maximum g_h and maximum ($d_h g_h$) are 3–4 times larger than those measured [28] on similar 0–3 composites and the data calculated in Fig. 2a,c. The improved figures of merit, by introducing controlled porosity, are due to the increased compliance and reduced permittivity of the polymer phase. Although the maxima determined take place at ceramic volume fractions $m_{\text{ceram}} \ll 1$, this result holds true at numerous variations of t , n , m_p , or α_{sa} , as shown in Table 3. These results enable us to conclude that piezoelectric sensitivity of the 0–0–3 composite at $h \rightarrow 1$ is highly dependent on both the porosity m_p and the ratio of semiaxes α_{sa} related to the disk-like pores (2). The parameters g_h , $d_{33}g_{33}$ and $d_h g_h$ are less dependent on t and n at the condition $h \rightarrow 1$ since t , n and h describe linear dimensions of the isolated and high stiffness piezoceramic inclusion irrespective of the medium surrounding this inclusion.

Thus, our study of the 0–3 and 0–0–3 piezocomposites based on modified PbTiO_3 makes it possible to predict the concentration dependences of the effective parameters (g_h , $d_{33}g_{33}$, $d_h g_h$, etc.) and

establish important extreme points of these parameters. Due to the lack of connectivity, piezoelectric strain constants such as d_{33} and d_h are low, but the reduced permittivity results in enhanced piezoelectric voltage constants such as g_{33} and g_h . Therefore 0–3 composites are suitable to sensing applications (e.g. hydrophones), rather than active transducers. It is important to note that high piezoelectric sensitivity depends not only on the microgeometry of the composite, but also on the volume fraction of the ceramic and the presence of elongated porosity in the polymeric phase, which is an area that has not been studied in detail. The common feature of the 0–3 based composites studied in this section is that the relatively small volume fraction of the ceramic component can be regarded as a necessary condition for high piezoelectric sensitivity.

4. PbTiO_3 -based composites with 3–3 connectivity

The next stage in the development of composite structures requires the creation of a piezoceramic–polymer composite that can provide extremely high piezoelectric sensitivity with a relatively high piezoceramic volume fraction (m_{ceram}), i.e., the conditions $g_h^c/g_h^m \gg 1$, $d_{33}^c g_{33}^c / (d_{33}^m g_{33}^m) \gg 1$, $d_h^c g_h^c / (d_h^m g_h^m) \gg 1$, and $m_{\text{ceram}} \sim 1 - m_{\text{ceram}}$ are fulfilled simultaneously.

An important method of increasing the piezoelectric sensitivity consists of increasing the connectivity of the piezoactive element, as is the case in 1–3 piezocomposite based systems. In a 3–3 composite the degree of piezoceramic connectivity is increased to three dimensions to create interpenetrating piezoceramic and polymer phases and enables high piezoelectric activity, such as d_{33} or d_h and relatively low dielectric permittivity (ϵ_{33}^T). A typical Banno type unit cell for a 3–3 geometry is shown in Fig. 4a, where the interpenetrating piezoelectric and polymer regions are indicated.

As the permittivity of the piezoelectric phase is significantly greater than that of the polymer it will dominate the effective permittivity of the composite. By examination of Fig. 4b, the piezoelectric column parallel to the poling direction (OX_3) contributes to ϵ_{33}^T of the composite (volume 1). The other volumes contribute little to the effective permittivity since they consist of either low permittivity polymer (volume 2) or a piezoelectric phase in series with a polymer in the OX_3 direction (volumes 3 and 4). The dielectric constant can therefore be approximated [10] to

$$\epsilon_{33}^{T, \text{composite}} = \epsilon_{33}^{T, \text{PbTiO}_3} \cdot m^{\text{PbTiO}_3} \quad (3)$$

where $\epsilon_{33}^{T, \text{composite}}$ is the effective permittivity at constant stress of the composite, $\epsilon_{33}^{T, \text{PbTiO}_3}$ is the

permittivity at constant stress of the piezoelectric phase, $m^{\text{PbTiO}_3} = L^2 / (L + l)^2$ is the volume fraction of piezoelectric phase contributing to the composite permittivity.

To calculate the composite d_{33} piezoelectric strain coefficient, the fraction of force experienced by the active piezoelectric phase must be calculated. If a force, F_3 , is applied in the OX_3 -direction, the total force is distributed through four volumes indicated in Fig. 4b. The polymer phase will experience less force, being of significantly higher compliance than the piezoceramic phase and has led to the assumption in some models of complete stress transfer into the active ceramic phase [10]. However, the actual distribution of the force between the four volumes depends on the respective compliances of the volumes and the cross sectional area of each volume. For volume 1, the compliance s_{33}^{V1} is that of the monolithic piezoelectric material, defined as $s_{33}^{\text{PbTiO}_3}$ and the area $a^{V1} = L^2$. For volume 2, the compliance s_{33}^{V2} is that of the polymer, defined as s_{33}^{polymer} and the area is $a^{V2} = l^2$. Volumes 3 and 4 are identical in geometry and consist of a polymer phase and a piezoelectric phase connected in series in the OX_3 -direction. The area of both volumes is $a^{V3} = a^{V4} = L \cdot l$ and the compliance of the volumes in the OX_3 direction can be calculated using a series model using,

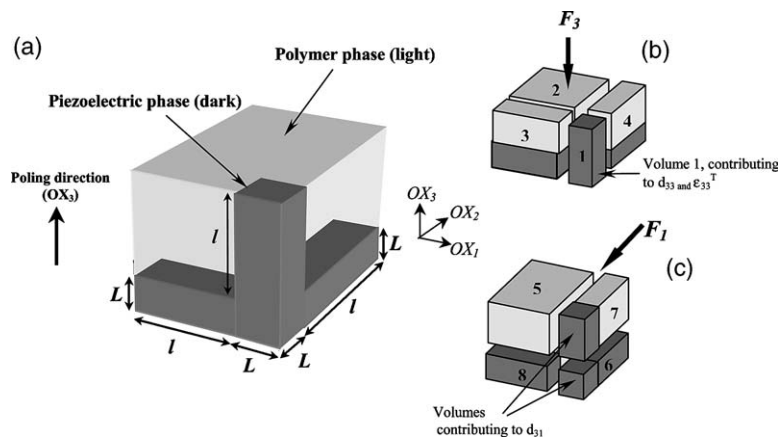


Fig. 4. Unit cell and distribution of forces in the 3–3 piezocomposite (a) model representing an interpenetrating 3–3 piezocomposite structure, the piezoceramic volume fraction is dependent on the piezoelectric column width (L) and length (l); (b) force in OX_3 direction (F_3) is distributed through volumes 1–4, volume 1 contributes to d_{33} and ϵ_{33}^T ; (c) force in OX_1 direction (F_1) is distributed through the volumes 5–8, cube in volume 6 and piezoelectric phase in volume 7 contributes to d_{31} .

$$s_{33}^{V3} = s_{33}^{V4} = m^{V3} s_{33}^{\text{PbTiO}_3} + (1 - m^{V3}) \cdot s_{33}^{\text{Polymer}} \quad (4)$$

$$= \frac{L \cdot s_{33}^{\text{PbTiO}_3} + l \cdot s_{33}^{\text{Polymer}}}{(L + l)}$$

where m^{V3} is the volume fraction of piezoelectric phase in volume 3, s_{33}^{V3} is the compliance of volume 3, s_{33}^{V4} is the compliance of volume 4. At high or intermediate volume fractions of ceramic, only volume 1 can be considered to contribute to the effective d_{33} of the composite. Volume 2 consists only of a passive polymer phase while the piezoelectric phases in volumes 3 and 4 are in series with the polymer in the OX_3 direction, which results in a negligible contribution to the d_{33} .

The d_{33} of a the 3–3 piezocomposites structure can therefore be calculated [10,11] from the formula below,

$$d_{33}^{\text{Composite}} = d_{33}^{\text{PbTiO}_3}$$

× fraction of load experienced by volume 1

$$= d_{33}^{\text{PbTiO}_3} \cdot \frac{L^2}{s_{33}^{\text{PbTiO}_3}} \left[\frac{L^2}{s_{33}^{\text{PbTiO}_3}} + \frac{l^2}{s_{33}^{\text{Polymer}}} + \frac{2 \cdot L \cdot l \cdot (L + l)}{L \cdot s_{33}^{\text{PbTiO}_3} + l \cdot s_{33}^{\text{Polymer}}} \right]^{-1} \quad (5)$$

By varying the values on L and l , the d_{33} of the composite can be calculated as a function of the ceramic volume fraction of ceramic. The same procedure is undertaken to calculate the d_{31} piezoelectric charge coefficient of the composite [10]. Consider a force acting in the OX_1 direction, which is distributed through the four volumes in Fig. 4c. The volume of active material contributing to the composite d_{31} is the cube in volume 6, as indicated in Fig. 4c (the remainder of volume 6 is neglected since it is in series in the OX_3 -direction with a polymer) and the piezoelectric phase in volume 7. The d_{31} of the unit cell is therefore,

$$d_{31}^{\text{Composite}} = d_{31}^{\text{PbTiO}_3} \cdot \frac{L}{(L + l)}$$

× fraction of force experienced by volumes 6 and 7

$$= d_{31}^{\text{PbTiO}_3} \cdot \frac{L}{(L + l)} \left[\frac{L \cdot l \cdot (L + l)}{L \cdot s_{11}^{\text{PbTiO}_3} + l \cdot s_{11}^{\text{Polymer}}} + \frac{L^2}{s_{11}^{\text{PbTiO}_3}} \right]$$

$$\left[\frac{l^2}{s_{11}^{\text{Polymer}}} + \frac{2L \cdot l \cdot (L + l)}{L \cdot s_{11}^{\text{PbTiO}_3} + l \cdot s_{11}^{\text{Polymer}}} + \frac{L^2}{s_{11}^{\text{PbTiO}_3}} \right]^{-1} \quad (6)$$

From Eqs. (3)–(6), the parameters ϵ_{33}^T , d_h and g_h can be calculated as a function of ceramic volume fraction and materials properties. All calculations were made for 3–3 PbTiO_3 -based piezoceramic–polymer composites using the data in Table 1 with a polymer 10 times more compliant than the ceramic phase ($s_{\text{ab}}^{\text{Polymer}} = 10s_{\text{ab}}^{\text{PbTiO}_3}$). The most important results are graphically represented in Fig. 5 and show ϵ_{33}^T , d_h , g_h and $d_h \cdot g_h$ as a function of ceramic volume fraction for PbTiO_3 -based piezoceramics based on modified PbTiO_3 , PCR-62, PCR-63 and $\text{Pb}(\text{Zr}_{1-x}\text{Ti}_x)\text{O}_3$ where $x = 0.1, 0.2, 0.3$ and 0.4 .

As would be expected, there is a gradual reduction in ϵ_{33}^T as the low permittivity polymer replaces the piezoceramic of high ϵ_{33}^T (Fig. 5a). Fig. 5b shows that the d_h reaches a maximum at polymer volume fractions in the 0.4–0.5 range for the PCR-63, PCR-62 and different solid solutions of $\text{Pb}(\text{Zr}_{1-x}\text{Ti}_x)\text{O}_3$. The highest composite d_h values are achieved using piezoceramic material with the highest d_{33} values (PCR-62 and PCR-63). In 1–3 composites the maximum in d_h is generally achieved at higher polymer volume fractions of 0.7–0.8 [7]. The mechanism by which d_h increases for 3–3 composites is similar to that for 1–3's [3,5,15,16]; whereby the composite structure leads to decoupling of stress and a large reduction in the d_{31} relative to the d_{33} piezoelectric coefficient. It is for this reason that the ceramics which experience the greatest enhancement of d_h relative to that of the bulk value are those with a small anisotropy factor $-d_{33}/d_{31}$ (i.e. a relatively high $-d_{31}$), such as PCR-62 and PCR-63 (Fig. 5b and Table 1). For the modified PbTiO_3 , no increase in d_h is observed (Fig. 5b) as the bulk material inherently exhibits a high $-d_{33}/d_{31}$ ratio due to its relatively high d_{33} (51 pCN^{-1}), low d_{31} (-4.4 pCN^{-1}) and initial high d_h value. Incorporating polymer into this modified PbTiO_3 merely serves to gradually decrease d_{33} and the associated the d_h value (Fig. 5b). For a particular piezoceramic/polymer composite system, the reduction in d_{31} relative to d_{33} (and the resulting increase in d_h) is greater for 3–3 composites than

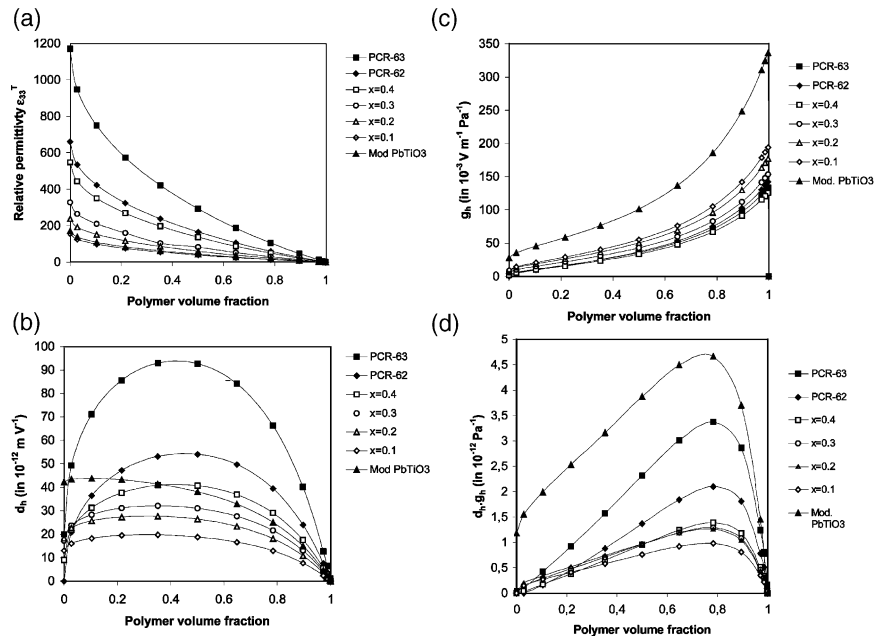


Fig. 5. Effective parameters ϵ_{33}^T (a), d_h (b), $d_{33}g_{33}$ (b) g_h (c), and d_hg_h (d) calculated for the 3–3 composite “PbTiO₃-based piezoceramic – polymer” with elements of microgeometry shown in Fig. 4. Piezoceramics presented include modified PbTiO₃, PCR-62, PCR-63 and Pb(Zr_{1-x}Ti_x)O₃ where $x = 0.1, 0.2, 0.3$ and 0.4 (see Table 1).

1–3 composites. This is due to relatively high stiffness of the ceramic along the OX_1 and OX_2 axes of the 3–3 composite (Fig. 4a), which acts to stiffen the structure in these directions and reduce d_{31} . It is for this reason that top and bottom metallic cover plates are used in 1–3 composites, i.e. to stiffen the structure the OX_1 and OX_2 directions and increase d_h [7].

The g_h values for all the 3–3 composites increase as polymer is incorporated into the 3–3 structure (Fig. 5c). This is generally a consequence of the increase in d_h and decrease in the permittivity of the composite. The highest g_h is observed for the modified PbTiO₃ based composite, due to the relatively low permittivity (170) and relatively high d_{33} coefficient (51 pCn⁻¹). The HFOM (d_hg_h) reaches a maximum at volume fractions of approximately 0.8 and, unlike 0–3 composites, large increases are observed compared to the d_hg_h of the bulk material (Fig. 5d). As an example, a PCR-63/polymer 3–3 composite exhibits a maximum d_hg_h of 3.4 pPa⁻¹ (Fig. 5d), while for the bulk material it is 0.04 pPa⁻¹. A similar maximum is observed for 1–3 composites, where the maximum is located at

slightly higher polymer volume fractions of 0.9 [7]. The 3–3 connectivity leads to large d_{33} and d_h values compared to 0–3 composites which enables both signal generation and signal sensing applications to be considered, assuming the composite has an optimum architecture. The optimum architecture in terms of choice of ceramic volume fraction and choice of piezoceramic depends on the application and the appropriate figure of merit that needs to be maximised.

5. Conclusions

Results of modelling of piezoactive composites of 0–3 and 3–3-types have been presented in order to determine the important factors influencing high piezoelectric sensitivity at different elements of microgeometry. For both connectivity cases considered the models predict significant improvements in effective piezosensitivity parameters, such as g_h , $d_{33}g_{33}$ and d_hg_h , compared to those of dense monolithic PbTiO₃ based materials. The greatest benefits in d_h for the 3–3 materials are achieved at

high ceramic volume fractions using materials with high d_{33} and small $-d_{33}/d_{31}$ ratios, although in all cases the reduction in dielectric permittivity at low ceramic volume fractions leads to large increases in g_h . High figures of merit are achieved compared to 1–3 composites, due to the stiff ceramic interconnected in the OX_1 and OX_2 directions. The 0–3 materials are less sensitive to the anisotropy factor but modelling has shown that piezoelectric sensitivity can be increased by modification of the matrix, for example by the formation of a system of elongated pores in the polymer media or using “plate like” inclusions aligned in the poling direction. The models presented enable 0–3 and 3–3 composites to be optimised depending on the application and the figure of merit that needs to be maximised. The important factor that influences piezoelectric sensitivity is associated with the arrangement of the ceramic component: in all these composite structures there are ceramic elements that are lengthy along the poling axis OX_3 which promote the effective redistribution of the internal electric and mechanical fields.

Acknowledgements

The authors would like to thank Prof. Dr. A. V. Turik and Prof. Dr. A. E. Panich (Rostov State University, Russia) for their constant interest in the research problems. The work was partially supported by the administration of the Rostov State University (Grants-in-aid Nos. 11.01.02f and 11.01.03f on basic research) and the UK Engineering and Physical Sciences Research Council (EPSRC).

References

- [1] Mendiola J, Jimenez B. *Ferroelectrics* 1984;53:159.
- [2] Grekov AA, Kramarov SO, Kuprienko AA. *Ferroelectrics* 1987;76:43.

- [3] Grekov AA, Kramarov SO, Kuprienko AA. *Mekhanika Kompositnykh Materialov* 1989;N 1:62 In Russian.
- [4] Cao W, Zhang QM, Cross LE. *IEEE Trans. Ultrason., Ferroelec., a. Freq. Contr.* 1993;40:103.
- [5] Taunamang H, Guy IL, Chan HLW. *J. Appl. Phys.* 1994;76:484.
- [6] Li L, Sottos NR. *J. Appl. Phys.* 1995;77:4595.
- [7] Bennett J, Hayward G. *IEEE Trans. Ultrason., Ferroelec., a. Freq. Contr.* 1997;44:565.
- [8] Gibiansky LV, Torquato S. *J. Mech. Phys. Solids.* 1997;45:689.
- [9] Sigmund O, Torquato S, Aksay IA. *J. Mater. Res.* 1998;13:1038.
- [10] Bowen CR, Perry A, Kara H, Mahon SW. *J. Europ. Ceram. Soc.* 2001;21:1463.
- [11] Bowen CR, Perry A, Stevens R, Mahon S. *Integ. Ferroelec.* 2001;32:1025.
- [12] Glushanin SV, Topolov V, Yu. *J. Phys. D: Appl. Phys.* 2001;34:2518.
- [13] Newnham RE, Skinner DP, Cross LE. *Mater. Res. Bull.* 1978;13:525.
- [14] Newnham RE. *MRS Bull.* 1997;22:20.
- [15] Topolov VYu, Turik AV. *Tech. Phys. Lett.* 2001;27:81.
- [16] Topolov VYu, Turik AV. *Tech. Phys.* 2001;46:1093.
- [17] Turik AV, Topolov VYu, Aleshin VI. *J. Phys. D: Appl. Phys.* 2000;33:738.
- [18] Topolov VYu. *Electromechanical effects in heterogeneous ferroelectrics and related materials. Thes Dr Sci (Phys & Math)* Rostov-on-Don: Rostov State University; 1999. p. 417 [in Russian].
- [19] Ikegami S, Ueda T, Nagata T. *J. Acoust. Soc. Amer.* 1974;50:1060.
- [20] Dantsiger AY, Razumovskaya ON, Reznitchenko LA et al. *Highly effective piezoceramic materials (Handbook)*. Rostov-on-Don: Kniga, 1994 p. 32 [in Russian].
- [21] Gorish AV, Dudkevich VP, Kupriyanov MF, Panich AE, Turik AV. *Piezoelectric Device Designing. Physics of ferroelectric ceramics, vol 1*. Moscow: Publishing company of the journal “Radiotechnique”, 1999 p. 368, (in Russian).
- [22] Schaumburg H, editor. *Keramik*. Stuttgart: BG Teubner; 1995. 650 p.
- [23] Topolov VYu, Bondarenko EI, Turik AV, Chernobabov AI. *Ferroelectrics* 1993;140:175.
- [24] Banno H. *Ceram. Bull.* 1987;66:1332.
- [25] Levassort F, Topolov VYu, Lethiecq M. *J. Phys. D: Appl. Phys.* 2000;33:2064.
- [26] Levassort F, Lethiecq M, Certon D, Patat F. *IEEE Trans. Ultrason., Ferroelec., a. Freq. Contr.* 1997;44:445.
- [27] Dunn ML. *J. Appl. Phys.* 1995;78:1533.
- [28] Garner GM, Shorrocks NM, Whatmore RW et al. *Ferroelectrics* 1989;93:169.